Structural, optical and antibacterial characteristics of CdO nanostructure prepared via simple method

Abdullah Ahmed Ali Ahmed [a,*], Shayefe A. Issa [a], Sultan A. Al-Marbie [a], Mohammed A. Al-Geraei [a], Hajer A. Al-Mtouakell [a], Seham A. Al-Mangathi [a], Jameel M. Abduljaleel [b], Ahmed A. Qaid [c]

[a] *Department of Physics, Faculty of Applied Science, Thamar University, Dhamar 87246, Yemen*

[b] *Department of Biology, Faculty of Applied Science, Thamar University, Dhamar 87246, Yemen*

[c] *Department of Chemistry, Faculty of Applied Science, Thamar University, Dhamar 87246, Yemen*

[*] *Corresponding author E-mail : abdullah2803@gmail.com*

DOI: https://doi.org/10.56807/buj.v2i2.51

Abstract

CdO nanostructure was synthesized using the simple co-precipitation method at three concentrations of ethylene glycol (EG) (0.01, 0.1 and 1 M) as stabilization materials. The prepared samples were calcined at 450 °C for 3 h. The structural properties of samples were studied using X-ray diffraction (XRD). The XDR patterns showed good crystallinity of CdO samples and the crystallite size increased from 32.5 nm to 35 nm as the EG concentration increased from 0.01 M to 1 M. The optical properties of CdO samples were investigated using UV-visible spectroscopy. The absorbance spectra of the prepared samples showed UV absorption band with cut-off wavelength less than 271 nm. The optical band gap decreased from 4.09 eV to 3.59 eV as crystallite size increased from 32.5 nm to 35 nm due to the nanostructure nature of the prepared samples. Antibacterial activities of CdO samples were evaluated against three types of bacteria (Staphylococcus aureus, Escherichia coli and Pseudomonas aeruginosa) and the zone range of the inhibition (9 – 14 mm). The reactive oxygen species (ROS), such as, superoxide anion radical, hydroxyl radical and hydrogen peroxide have been generated on the surface of the CdO nanoparticles. The released Cd^{2+} from the surfaces of the CdO nanostructure and ROS come into contact with the bacterial cell membranes and cause membrane and protein denaturation damage.

Keywords : *CdO nanostructure; Co-precipitation method; Structural properties; Optical properties; Antibacterial activities*

دراسة الخواص التركيبية والبصرية والفعالية المضادة للبكتريا لمركب اكسيد الكاديوم النانوني المحضر بطريقة بسيطة

الملخص

في هذا الدراسة، تم تحضير مركب اكسيد الكاديوم النانوني بطريقة الترسيب البسيطة وذلك باستخدام ثلاثة تراكيز من بولي ايثلين الجلايكول (0.01 و 0.1 و 1 مولار) للحصول على تغيير في حجم المركب النانوني. لقد تم تكسير الراسب المتكون من التجربة عند درجة حرارة 450 درجة مئوية لمدة 3 ساعات في وجود الهواء. تم دراسة الخواص التركيبية للمركبات المحضرة باستخدام جهاز حيود الاشعة السينية وقد اظهرت نتائج الدراسة ان المركبات المحضرة لها تركيب متعدد التبلور ذو تركيب مكعبي متمركز الوجه. كما اظهرت الدراسة ان الحجم البلوري لأكسيد الكاديوم يزيد من 32.5 الى 35 نانومتر بزيادة تركيز البولي ايثلين الجلايكول من 0.01 الى 1 مولار. تم دراسة الخواص البصرية للمركبات المحضرة باستخدام جهاز مطيافية الفوق بنفسجية و المنطقة المرئية. لقد اظهرت اطياف الامتصاصية ان العينات قيد الدراسة تملك اطوال موجية قطع ضمن المنطقة فوق البنفسجية. كما اظهرت قيم فجوة الطاقة للمركبات انها تقل من 4.09 الى 3.59 الكترون فولت عند زيادة الحجم البلوري لتلك المركبات من 32.5 الى 35 نانومتر وهذا يعود الى الخاصية النانونية التي تميزت بها العينات قيد الدراسة. تم دراسة الفعالية المضادة للبكتريا للعينات المحضرة على ثلاثة انواع من البكتيريا المعدية (*Staphylococcus aureus*, *Escherichia coli* and *Pseudomonas aeruginosa*). لقد اظهرت اختبارات

الفعالية المضادة للبكتريا ان عرض الهالات المتكونة بسبب اضافة العينات قيد الدراسة تتراوح بين 9 و 14 مليمتر. يمكن تفسير تكون تلك الهالات والتي تعبر عن قتل البكتريا من انتاج مركبات الاكسجين الفعالة (ROS) مثل جذور البيروكسيد الهيدروجين و جذور السوبر بيروكسيد. يتم توليد تلك الجذور على سطح مركبات اكسيد الكادميوم النانوية. بالإضافة لتلك الجذور المتولدة، فان ايونات الكادميوم تظهر عند سطح مركبات اكسيد الكادميوم النانوية والتي تعمل كلها (الجذور وايونات الكادميوم) على الاتصال بجدار الخلية البكتيرية ومن ثم تسبب اضرار بليغه له. هذا يؤدي بدوره الى دخول الجذور الفعالة المتولدة وتدمير البروتينات وبقية المكونات الحيوية للخلية البكتيرية مما يسبب موتها في النهاية.

1. Introduction

Nanoparticles ranging in size from 1 to 100 nm have been widely used in biotechnology, pharmacology and medicine due to their novel physicochemical properties (Morones *et al.*, 2005; Niemeyer, 2001; Whitesides, 2005). Extremely amazing activities of nanoparticles have enormous potential for emphasizing their use in human (Heiligtag & Niederberger, 2013; Mullai *et al.*, 2013). The bacterial contamination of food can occur before, during, and after the preparation of food. The toxins released by bacteria in contaminated food can be highly harmful to human health. Moreover, foodborne pathogens have recently become the most common global public health problem (Pinilla & Brandelli, 2016; Wang *et al.*, 2014). Therefore, in order to overcome this problem, it is necessary to develop novel inorganic antibacterial compounds to combat *E. coli*, *P. aeruginosa* and *S. aureus*.

Semiconductor cadmium oxide (CdO) nanostructures have a direct wide band gap (4.05 eV), have a polycrystalline structure, and are an n-type of semiconductor. For the bulk CdO, it has a direct band gap of 2.5 eV and the indirect band gap of 1.98 eV (Kuo & Huang, 2006; Lu *et al.*, 2008). CdO nanostructures offer many applications such as photovoltaic cells, gas sensors, transparent electrodes, solar cells, laser, infrared reflectors, liquid crystal displays, anti-reflection coating and have biomedical applications (Shukla *et al.*, 2012; Sivakumar *et al.*, 2015; Thema *et al.*, 2015; Thovhogi *et al.*, 2016). CdO nanostructures are of a great interest research area in the medical and pharmaceutical field, with several applications, including attack and elimination of cancer cells, drug delivery, identification and location of tumors, inhibition of bacterial cells, and magnetic resonance imaging (Heidari & Brown, 2015; Lim *et al.*, 2015).

Recently, glucose encapsulated cadmium oxide nanoparticles were synthesized and used to improve the over conventional approaches to cancer and drug resistance. and in therapeutic intervention against advanced glycation end products (AGEs). Metal oxide NPs can inhibit cancerous cells, bacteria, and fungi. Moreover, the use of CdO nanoparticles could be therapeutically beneficial in the treatment of cancer, bacterial infections, and in treating glycation (Zahera *et al.*, 2020). Demir *et. al.*, have synthesized 10 nm CdO core-polyethylene glycol stabilized nanoparticles and used for evaluation of CdO nanoparticles' cytotoxicity and genotoxicity using *in vitro* assays (Demir *et al.*, 2020). The effect of CdO nanoparticles on the immune response, renal and intestine oxidative stress, blood antioxidant defense, renal fibrotic response, bone density and mineral content has been investigated via six-week-old female ICR mice (Tulinska *et al.*, 2020).

In this work, CdO nanostructures were prepared by simple coprecipitation method using different concentration of EG (0.01, 0.1 and 1 M) as stabilization materials. The final CdO nanostructures were obtained as the calcination process at 450 °C for 3 h. The structural and optical band gap energies of prepared samples were explained. Antibacterial activities of CdO samples were evaluated against three types of bacteria (*Staphylococcus aureus*, *Escherichia coli* and *Pseudomonas aeruginosa*).

2. Experimental

2.1 Materials

The starting chemicals of cadmium chloride ($CdCl_2$) (System, 99%), ethylene glycol (System, 99%) and sodium hydroxide (NaOH) (System, 98%) were used without further purification.

2.2 Synthesis of CdO nanostructures

Firstly, 0.1 M of cadmium chloride (solution A) and 0.1 M of sodium hydroxide

(solution B) were prepared separately using continues stirrer for 15 min at room temperature. 0.01, 0.1 and 1 M of ethylene glycol (EG) were also prepared separately. 10 ml of 0.01 M EG was added to 100 ml of solution B under continues stirrer for 1 h at room temperature to obtain homogenous solution (solution C). Then, 20 ml of solution A was added to solution C under continues stirrer for 3 h at room temperature to obtain brownish colored solution and denoted as solution 0.01. The last two steps were repeated for 0.1 and 1 M EG and denoted as solution 0.1 and solution 1, respectively. The final 3 brown solutions were left on Lab bench at room temperature for 48 h to get white precipitate. Three white precipitates were centrifuged and washed one time by acetone and another two times by methanol and dried in an oven at 80 °C for one day to obtain the final white precipitates. Finally, the 3 precipitates were calcined at 450 °C for 3 h to obtain brown fine powder and the calcined samples were labelled as CdO-0.01, CdO-0.1 and CdO-1, respectively. Heating was done in an electric tubular furnace at atmospheric pressure in a ceramic boat holder. As the heat treatment was completed, the sample was left to cool to room temperature and kept in a sample bottle for further characterizations.

2.3 Antibacterial Activity

The antibacterial activity of CdO nanostructures was examined against three bacteria (*Staphylococcus aureus*, *Escherichia coli* and *Pseudomonas aeruginosa*) using disc diffusion method. The bacterial strains were grown in nutrient broth at 37 °C in an orbital shaker. Bacterial culture was swabbed over the surface of Muller Hinton Agar (MHA) with concentration of (1×10^8 CFU/mL) and allowed to dry for a few minutes. For positive control, Gentamicin antibiotic was used while, for negative control, distilled water was used. Discs loaded with CdO nanostructures (0.5, 1 and 2 mg/disc) were placed on the surface using sterile forceps followed by incubating the plates at 37 °C for 18 h. The zone of inhibition (ZOI) was measured in each plate in (mm) unit (Carroll *et al.*, 2015).

2.4 Characterizations

The structural properties of prepared samples were investigated using x-ray diffraction (XRD) technique (XD-2 x-ray diffractometer using CuKα (λ = 1.54 Å) at 36 kV and 20 mA, China) in Yemeni Geological Survey and Minerals Resources Board (YGSMRB). The optical properties included the absorbance spectra were measured using a UV-VISIBLE spectrophotometer (50conc) at room temperature in the range of (200 – 900 nm). Antibacterial activity of prepared samples was examined in the microbiological lab at Faculty of Applied Science.

3. Results and Discussion

3.1 Structural Properties

Fig. 1 exhibits XRD patterns of three CdO prepared samples. The observed diffraction patterns showed strong reflections from the (111), (200), (220), (311) and (222) planes could be indexed to the face-centered-cubic (FCC) Monteponite structure of CdO. The prepared cubic phase of the polycrystalline Monteponite CdO (JCPDS card number 05-0640) is in agreement with previous literatures (Bazargan *et al.*, 2009; Ramazani & Morsali, 2011; Sone & Maaza, 2017). The crystallite size (D) at the highest reflection plane (111) of the prepared CdO nanostructures is calculated using Debye–Scherrer's equation:

$$\boldsymbol{D = \frac{K\lambda}{\beta \cos\theta}} \qquad (1)$$

where $\boldsymbol{\lambda}$ is the x-ray wavelength, $\boldsymbol{K}$ corresponds to the shape constant (0.9), $\boldsymbol{\theta}$ is the Bragg angle and $\boldsymbol{\beta}$ is the full width height maximum (FWHM) of the diffracted peak.

The calculated crystallite size of CdO nanostructures using Eq. 1 was listed in Table 1. The crystallite size of CdO samples decreased as a concentration of EG decreased. These results are in agreement with previous study (Manickathai *et al.*, 2008) which maybe attributed to the nature of the stating solution/ethylene glycol mixture. The lattice parameter was also listed in Table 1. Lattice parameter ($\boldsymbol{a}$) was calculated using relation, $\boldsymbol{a = d_{hkl}\sqrt{h^2 + k^2 + l^2}}$ (d_{hkl} is the

interplanar spacing and ***h, k*** and ***l*** are the miller indices).

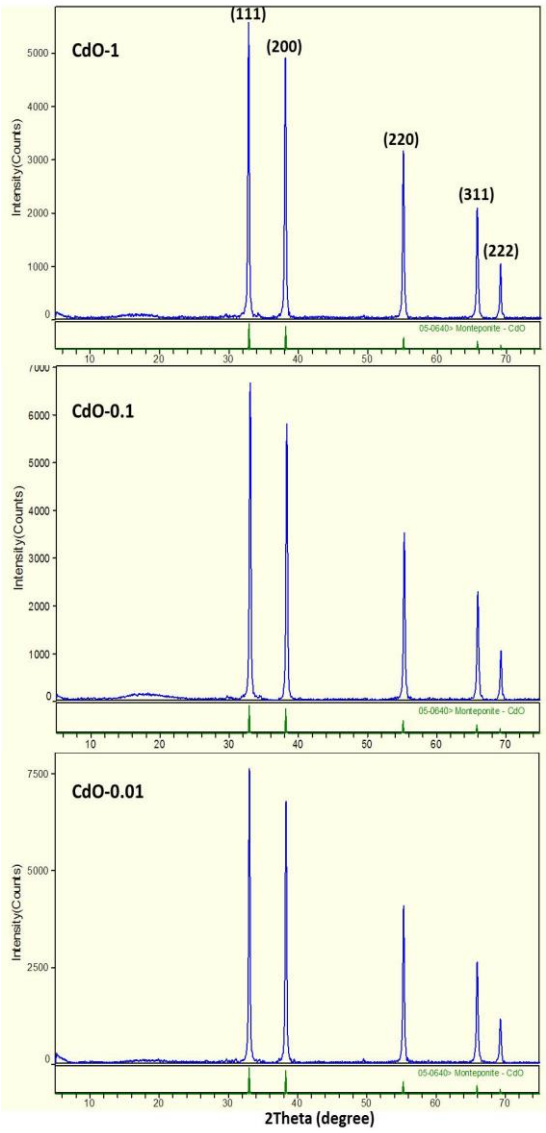

Figure 1. *XRD patterns of CdO-0.01, CdO-0.1 and CdO-1 nanostructures.*

Table 1: *The indexing of XRD for CdO nanostructures.*

Samples	Plane	d_{111} (Å)	a (Å)	D (nm)
CdO-1	(111)	2.7265	4.7224	35
CdO-0.1	(111)	2.7089	4.6920	34.1
CdO-0.01	(111)	2.7105	4.6947	32.5

3.2 Optical Properties

In this study, the optical properties were investigated for CdO samples which have a direct transition of an electronic excitation from the valance band (VB) to the conduction band (CB). Fig. 2 shows the absorbance spectra of the prepared samples which presented absorbance band at ultraviolet region. These results suggested that the prepared CdO could be used as UV filter/or detector. The cut-off wavelengths were 271, 275 and 277 nm for CdO-1, CdO-0.1 and CdO-0.01, respectively. Kumar *et al.*, (Kumar *et al.*, 2017) and Gowri *et al.*, (Gowri *et al.*, 2018) have presented cut-off wavelength at 298 and 297 nm, respectively, compared with the results of the current work, suggested blue shift due to reduce the crystallite size of the prepared CdO nanostructures.

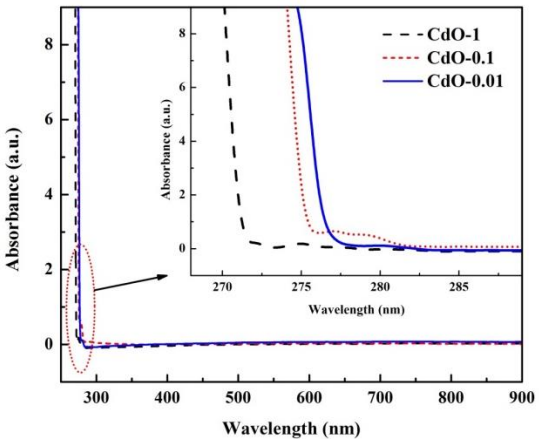

Figure 2. *Absorbance spectra of CdO samples.*

The optical absorption coefficient (α) is calculated from the absorption (A) and thickness of the sample cell (t = 1 cm) from following relation:

$$\alpha = \frac{2.303 * A}{t} \quad (2)$$

The direct optical band gap energy of CdO nanostructures can be calculated using Tauc's equation:

$$(\alpha . h\nu)^2 = C(h\nu - E_g) \quad (3)$$

where C is the characteristics parameter (free of photon energy) for this transition, h is the Planck's constant, ν is the frequency of light and E_g is the optical band gap energy. The variation of

$(\alpha.hv)^2$ versus (hv) is plotted and the straight line range of these plots are extended on (hv) axis to obtain the values of optical band gap of the samples.

Fig. 3 and Table 2 revealed that the prepared CdO samples have values of the optical band gap energy (E_g) higher than the bulk CdO (2.4 eV) due to the nanostructure nature of prepared materials. The current results are in good agreement with these studies (Barve *et al.*, 2014; Manickathai *et al.*, 2008) which found at values of 3.4 and 3.7 eV. The optical band gap (Eg) of prepared CdO nanostructure increased from 3.59 to 4.09 eV as the crystallite size decreased from 35 to 32.5 nm as shown in Fig. 4 which assigned to the weak quantum confinement of the prepared materials.

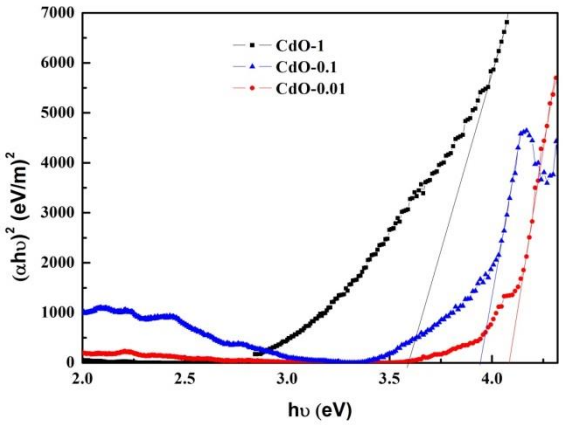

Figure 3. *Optical energy band gaps of CdO samples.*

Table 2: *Optical band gap energy (E_g) for CdO nanostructures.*

Samples	E_g (eV)
CdO-1	3.59
CdO-0.1	3.94
CdO-0.01	4.09

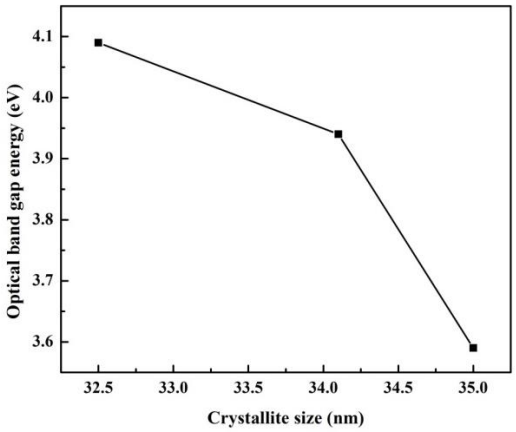

Figure 4. *Variation of energy band gap values versus the crystallite size of CdO nanostructures.*

3.3 Antibacterial activity

The antibacterial activity of CdO nanostructures was evaluated with three different concentrations (0.5, 1 and 2 mg/disc) against three bacteria (*Staphylococcus aureus*, *Escherichia coli* and *Pseudomonas aeruginosa*). It is well known that a superior antibacterial activity is obtained if the diameter of the antibacterial zone of inhibition is greater than 6 mm, but weak if the diameter is smaller than 6 mm. Fig. 5, Fig. 6 and Table 3 shows that the antibacterial activity of the CdO-1 sample was better because the antibacterial zone of inhibition was (9 – 14 mm) with all of the bacterial strains tested in this work. The other two samples (CdO-0.1 and CdO-0.01) didn't show significant antibacterial zone of inhibition which was found less than 1 mm as shown in Fig. 5 and Fig. 6. This explains that the larger particle size of CdO-1 (35 nm) has higher effective antibacterial activity more than others.

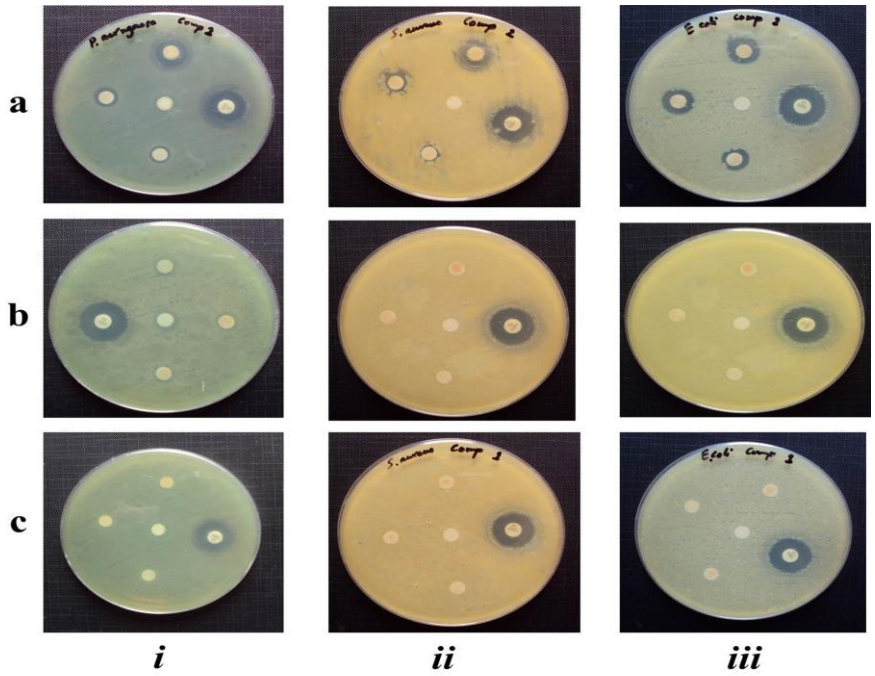

Figure 5. *Zones of inhibition obtained for: (a) CdO-1, (b) CdO-0.1, and (c) CdO-0.01 for (i) Pseudomonas aeruginosa, (ii) Staphylococcus aureus and (iii) Escherichia coli.*

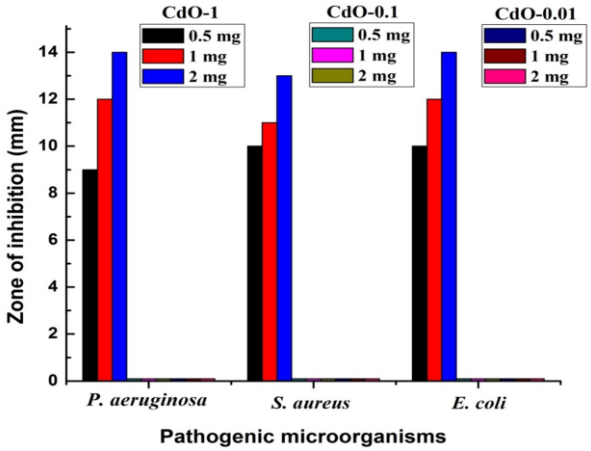

Figure 6. *Growth inhibition activity of different concentrations 0.5, 1 and 2 mg/ml of CdO nanostructures against various Gram negative bacterial pathogens.*

Table 3: *Antibacterial activity of CdO-1 sample against bacterial pathogenic organisms.*

Examined bacteria	Gram reaction	Zone of Inhibition (mm)			
		0.5 mg	1 mg	2 mg	ZOI, Ref
S. aureus	-ve	9 ± 0.2	12 ± 0.6	14 ± 0.4	11, (Xavier *et al.*, 2016)
E. coli	-ve	10 ± 0.4	11 ± 0.2	13 ± 0.6	12, (Xavier *et al.*, 2016)
P. aeruginosa	-ve	10 ± 0.3	12 ± 0.5	14 ± 0.8	22, (Karthik *et al.*, 2018)

The photogeneration of reactive oxygen species (ROS), such as , superoxide anion radical ($\dot{O}_2^-$), hydroxyl radical ($\dot{O}H$) and hydrogen peroxide (H_2O_2), on the surface of the metal oxide nanoparticles have been studied (Ezhilarasi *et al.*, 2016). Using reductive process, an electron excited by UV-Visible wavelengths and reacts with oxygen to generate ($\dot{O}_2^-$). Oxidative process was followed through the attraction of hole in the valence band with electrons of water or hydroxyl anions to produce the most reactive radical ($\dot{O}H$). Hydrogen peroxide (H_2O_2) was generated from the reaction between electron hole pairs and superoxide anions. The hydroxyl radical ($\dot{O}H$) and superoxide anion radical ($\dot{O}_2^-$) caused high damage to DNA, nucleic acids, carbohydrates and lipids. Among the ROS, H_2O_2 and $\dot{O}H$ are the most powerful oxidizing agents, which can directly penetrate the bacterial cell membrane to cause injuries and prevent the growth of cells, thereby leading to the bacteria death. The following equations present the generation of ROS:

$$CdO + h\nu \rightarrow h^+ + e^-$$

$$h^+ + H_2O \rightarrow \dot{O}H + H^+$$

$$e^- + O_2 \rightarrow \dot{O}_2^-$$

$$\dot{O}_2^- + H^+ \rightarrow H\dot{O}_2$$

$$H\dot{O}_2 + H^+ + e^- \rightarrow H_2O_2$$

Once the heavy metal ions Cd^{2+} released from the surfaces of the CdO nanostructure come into contact with the bacterial cell membranes, the negative charge on the cell membranes of bacteria and the positive charges of Cd^{2+} is mutually attracted, and Cd^{2+} penetrates the cell membrane to react with the thiol groups (**-SH**) of the proteins present on the bacterial cell surface. Cell membrane and protein denaturation damage can occur due to thiol binding and the protective function of the cell membrane is lost (Karthik *et al.*, 2018). Remarkably, in the present work, the CdO-1 sample at two concentrations of 1 and 2 mg/ml had a greater inhibitory effect on *Staphylococcus aureus* and *Escherichia coli* (12 and 14 mm, respectively) but the inhibitory effects on the another bacteria (*Pseudomonas aeruginosa*) was less to those of other works as presented in the last column of Table 3.

4. Conclusions

The structure of synthesized CdO nanostructure at three concentrations of EG (0.01, 0.1 and 1 M) via the simple co-precipitation was cubic phase of the polycrystalline Monteponite CdO with crystallite sizes of 35, 34.1 and 32.5 nm, respectively. The blue shift in cut-off wavelength of prepared samples was due to the smaller crystallites size of CdO. The optical band gap of samples (3.59 – 4.09 eV) was higher than the bulk CdO (2.5 eV) due to the nano-size nature of prepared CdO nanostructures. Antibacterial activities of CdO samples exhibited significance zone range of the inhibition (9 – 14 nm) against three types of bacteria (*Staphylococcus aureus*, *Escherichia coli* and *Pseudomonas aeruginosa*) due to the photogeneration of reactive oxygen species (ROS), such as, superoxide anion radical ($\dot{O}_2^-$), hydroxyl radical ($\dot{O}H$) and hydrogen peroxide (H_2O_2), on the surface of the CdO nanoparticles. Moreover, Cd^{2+} released from the surfaces of the CdO nanostructure came into contact with the bacterial cell membranes. Cell membrane and protein denaturation damage can occur due to thiol binding and the protective function of the cell membrane is lost.

References

[1]. Barve, A., Gadegone, S., Lanjewar, M., & Lanjewar, R. (2014). Synthesis and characterization of CdO nanomaterial and their photocatalyticactivity. *International Journal of Recent Innovations in Trends and Computer Communcation, 2*(9), 2806-2810.

[2]. Bazargan, A., Fateminia, S., Ganji, M. E., & Bahrevar, M. (2009). Electrospinning preparation and characterization of cadmium oxide nanofibers. *Chemical Engineering Journal, 155*(1-2), 523-527.

[3]. Carroll, K. C., Butel, J., & Morse, S. (2015). *Jawetz Melnick and Adelbergs Medical Microbiology 27 E*: McGraw-Hill Education.

[4]. Demir, E., Qin, T., Li, Y., Zhang, Y., Guo, X., Ingle, T., Yan, J., Orza, A. I., Biris, A., & Ghorai, S. (2020). Cytotoxicity and genotoxicity of cadmium oxide nanoparticles evaluated using in vitro assays. *Mutation Research/Genetic Toxicology and Environmental Mutagenesis*, 503149.

[5]. Ezhilarasi, A. A., Vijaya, J. J., Kaviyarasu, K., Maaza, M., Ayeshamariam, A., & Kennedy, L. J. (2016). Green synthesis of NiO nanoparticles using Moringa oleifera extract and their biomedical applications: Cytotoxicity effect of nanoparticles against HT-29 cancer cells. *Journal of Photochemistry and Photobiology B: Biology*, *164*, 352-360.

[6]. Gowri, S., Gopinath, K., & Arumugam, A. (2018). Experimental and computational assessment of mycosynthesized CdO nanoparticles towards biomedical applications. *Journal of Photochemistry and Photobiology B: Biology*, *180*, 166-174.

[7]. Heidari, A., & Brown, C. (2015). Study of composition and morphology of cadmium oxide (CdO) nanoparticles for eliminating cancer cells. *Journal of Nanomedicine Research*, *2*(5), 20.

[8]. Heiligtag, F. J., & Niederberger, M. (2013). The fascinating world of nanoparticle research. *Materials Today*, *16*(7-8), 262-271.

[9]. Karthik, K., Dhanuskodi, S., Gobinath, C., Prabukumar, S., & Sivaramakrishnan, S. (2018). Nanostructured CdO-NiO composite for multifunctional applications. *Journal of Physics and Chemistry of Solids*, *112*, 106-118.

[10]. Kumar, S., Ahmed, B., Ojha, A. K., Das, J., & Kumar, A. (2017). Facile synthesis of CdO nanorods and exploiting its properties towards supercapacitor electrode materials and low power UV irradiation driven photocatalysis against methylene blue dye. *Materials Research Bulletin*, *90*, 224-231.

[11]. Kuo, T.-J., & Huang, M. H. (2006). Gold-catalyzed low-temperature growth of cadmium oxide nanowires by vapor transport. *The Journal of Physical Chemistry B*, *110*(28), 13717-13721.

[12]. Lim, I., Shinde, D. V., Patil, S. A., Ahn, D. Y., Lee, W., Shrestha, N. K., Lee, J. K., & Han, S. H. (2015). Interfacial engineering of CdO–CdSe 3D microarchitectures with in situ photopolymerized PEDOT for an enhanced photovoltaic performance. *Photochemistry and photobiology*, *91*(4), 780-785.

[13]. Lu, H., Liao, L., Li, H., Tian, Y., Wang, D., Li, J., Fu, Q., Zhu, B., & Wu, Y. (2008). Fabrication of CdO nanotubes via simple thermal evaporation. *Materials Letters*, *62*(24), 3928-3930.

[14]. Manickathai, K., Viswanathan, S. K., & Alagar, M. (2008). Synthesis and characterization of CdO and CdS nanoparticles. *Indian Journal Of Pure & Applied Physics*, *46*, 561-564.

[15]. Morones, J. R., Elechiguerra, J. L., Camacho, A., Holt, K., Kouri, J. B., Ramírez, J. T., & Yacaman, M. J. (2005). The bactericidal effect of silver nanoparticles. *Nanotechnology*, *16*(10), 2346.

[16]. Mullai, P., Yogeswari, M., & Sridevi, K. (2013). Optimisation and enhancement of biohydrogen production using nickel nanoparticles–A novel approach. *Bioresource technology*, *141*, 212-219.

[17]. Niemeyer, C. M. (2001). Nanoparticles, proteins, and nucleic acids: biotechnology meets materials science. *Angewandte Chemie International Edition*, *40*(22), 4128-4158.

[18]. Pinilla, C. M. B., & Brandelli, A. (2016). Antimicrobial activity of nanoliposomes co-encapsulating nisin and garlic extract against Gram-positive and Gram-negative bacteria in milk. *Innovative food science & emerging technologies*, *36*, 287-293.

[19]. Ramazani, M., & Morsali, A. (2011). Sonochemical syntheses of a new nano-plate cadmium (II) coordination polymer as a precursor for the synthesis of cadmium (II) oxide nanoparticles. *Ultrasonics sonochemistry*, *18*(5), 1160-1164.

[20]. Shukla, M., Kumari, S., Shukla, S., & Shukla, R. (2012). Potent antibacterial activity of nano CdO synthesized via microemulsion scheme. *Journal of Materials and Environmental Science*, *3*(4), 678-685.

[21]. Sivakumar, S., Venkatesan, A., Soundhirarajan, P., & Khatiwada, C. P. (2015). Synthesis, characterizations and anti-bacterial activities of pure and Ag doped CdO nanoparticles by chemical precipitation method. *Spectrochimica Acta Part A: Molecular and Biomolecular Spectroscopy*, *136*, 1751-1759.

[22]. Sone, B., & Maaza, M. (2017). Room Temperature Green Synthesis of CdO Nanoparticles Using Aqueous Extracts of Callistemon Viminalis. *Journal of Nanomaterials and Molecular Nanotechnology*, *5*, 75-85.

[23]. Thema, F., Beukes, P., Gurib-Fakim, A., & Maaza, M. (2015). Green synthesis of Monteponite CdO nanoparticles by Agathosma betulina natural extract. *Journal of Alloys and Compounds*, *646*, 1043-1048.

[24]. Thovhogi, N., Park, E., Manikandan, E., Maaza, M., & Gurib-Fakim, A. (2016). Physical properties of CdO nanoparticles synthesized by green chemistry via Hibiscus Sabdariffa flower extract. *Journal of Alloys and Compounds*, *655*, 314-320.

[25]. Tulinska, J., Masanova, V., Liskova, A., Mikusova, M. L., Rollerova, E., Krivosikova, Z., Stefikova, K., Uhnakova, I., Ursinyova, M., & Babickova, J. (2020). Six-week inhalation of CdO nanoparticles in mice: The effects on immune response, oxidative stress, antioxidative defense, fibrotic response, and bones. *Food and Chemical Toxicology*, *136*, 110954.

[26]. Wang, C., Cheng, X., Zhou, X., Sun, P., Hu, X., Shimanoe, K., Lu, G., & Yamazoe, N. (2014). Hierarchical α-Fe2O3/NiO composites with a hollow structure for a gas sensor. *ACS applied materials & interfaces*, *6*(15), 12031-12037.

[27]. Whitesides, G. M. (2005). Nanoscience, nanotechnology, and chemistry. *Small*, *1*(2), 172-179.

[28]. Xavier, A. R., Ravichandran, A., Ravichandran, K., Mantha, S., & Ravinder, D. (2016). Sm doping effect on structural, morphological, luminescence and antibacterial activity of CdO nanoparticles. *Journal of Materials Science: Materials in Electronics*, *27*(11), 11182-11187.

[29]. Zahera, M., Khan, S. A., Khan, I. A., Sharma, R. K., Sinha, N., Al-Shwaiman, H. A., Al-Zahrani, R. R., Elgorban, A. M., Syed, A., & Khan, M. S. (2020). Cadmium oxide nanoparticles: An attractive candidate for novel therapeutic approaches. *Colloids and Surfaces A: Physicochemical and Engineering Aspects*, *585*, 124017.